Supporting Information

Finding Minimal Optimal Indent Separation for Polystyrene via Instrumental Nanoindentation and FEA Method

Chulin Jiang [1], Michael Davis [1] and Jurgita Zekonyte [2,*]

[1] School of Mechanical and Design Engineering, University of Portsmouth, Portsmouth PO1 3DJ, UK;

* Correspondence: Jurgita.Zekonyte@port.ac.uk;

Highlights

S1. Stress-Strain determination

S1.1. Stress and Strain for maximum depth h = 1 μm (Table S1.1, Figure S1.1)

S1.2. Stress and Strain for maximum depth h = 10 μm (Table S1.2, Figure S1.2)

S2. Mesh Convergence Study (Table S2, Figure S2.1, S2.2, S2.3)

S3. Experiment Analysis of Indents in a Matrix for $\boldsymbol{h = 10\mu m}$ (Figure S3.1, S3.2)

S4. Finite element analysis the maximum depth $\boldsymbol{h = 5\mu m}$ and $\boldsymbol{10\mu m}$ with three different orientations (Figure S4.1, S4.2)

S1. Stress-Strain determination

Compared against experimental data, a series of indentation stress constraint factor α is selected to get the matched loading-unloading curve with stress and strain. Three different indentation stress constraint factors are shown here to present the process. Material properties are determined as a function of depth.

S1.1. Stress and Strain for maximum depth h = 1 μm

The Young's modulus of polystyrene $E_{ps} = 4374MPa$ with depth $h = 1$μm is calculated from experimental interfacial modulus (or reduced modulus) Er = 4924 MPa. The stress and strain applied to ABAQUS using the indentation stress constraint factor α determined by the loading-unloading curve. Indentation strain ε_{ind} and effective indentation stress σ_{eff} with different indentation stress constraint factor α tabulated in Table S1.1 are applied to finite element analysis in order to identify the satisfactory curve. Figure S1.1 depicts the loading-unloading curves from ABAQUS compared with experimental cycle. The indentation strain and effective indentation stress with $\alpha = 1.87$ showing the highest accuracy are chosen for finite element analysis.

Table S1.1. Effective indentation stress and indentation strain with α and $h = 1$μm

ε_{ind}	σ_{eff} (MPa)		
	$\alpha = 1.80$	$\alpha = 1.87$	$\alpha = 1.90$
0	1.0	1.0	1.0
0.001	7.9	7.6	7.5
0.002	18.2	17.5	17.2
0.003	25.6	24.7	24.3
0.004	34.0	32.7	32.2
0.005	41.7	40.2	39.5
0.006	49.5	47.6	46.9
0.007	57.2	55.1	54.2
0.008	64.7	62.3	61.3
0.009	72.4	69.7	68.6
0.010	76.4	73.6	72.4
0.013	101.2	97.5	95.9
0.017	126.9	122.2	120.2
0.019	148.6	143.0	140.7

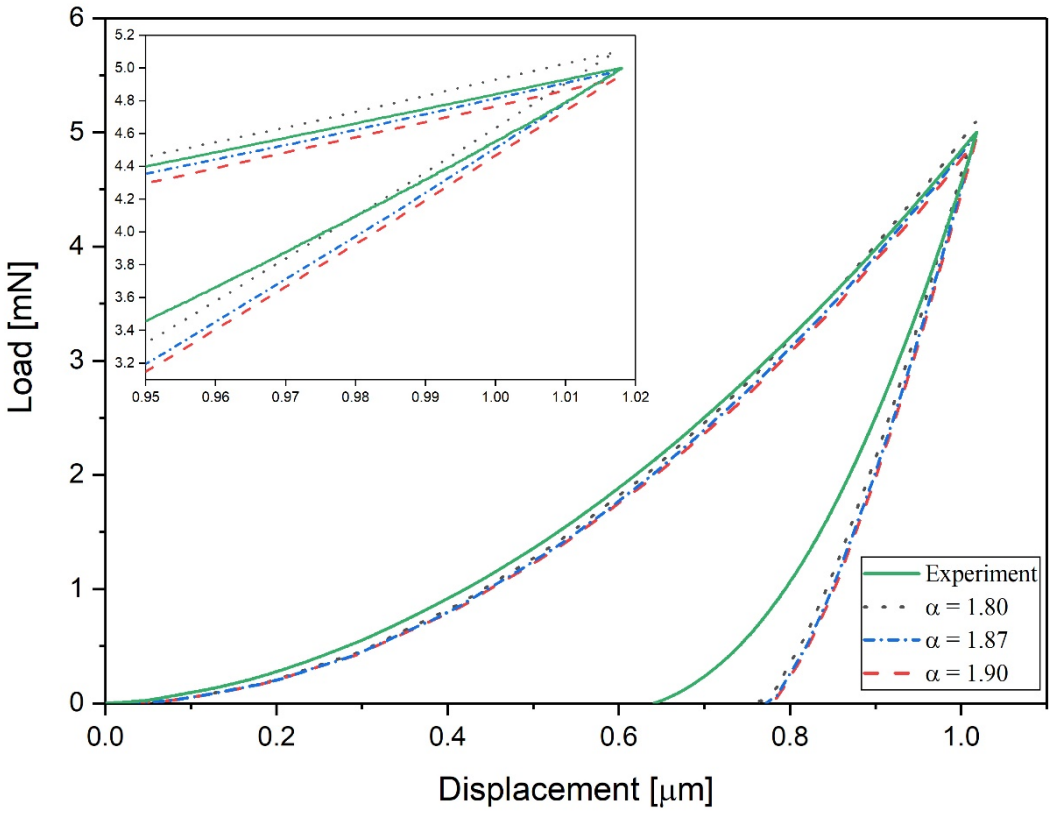

Figure S1.1. Loading-unloading curves with $h = 1\mu m$ from experiment and ABAQUS with different α.

S1.2. Stress and Strain for maximum depth h = 10 μm

The Young's modulus of polystyrene $E_{ps} = 3840MPa$ with depth $d = 10\mu m$ is calculated from experimental interfacial modulus, Er = 4326 MPa. Indentation strain ε_{ind} and effective indentation stress σ_{eff} with different indentation stress constraint factor α tabulated in Table S1.2 are applied to finite element analysis. The loading-unloading curves from ABAQUS are compared with experimental curve shown in Figure S1.2. The indentation strain and effective indentation stress with $\alpha = 3$ showing the highest accuracy are chosen for finite element analysis with depth $d = 10\mu m$.

Table S1.2. Effective indentation stress and indentation strain with different α and $h = 10\mu m$

ε_{ind}	σ_{eff} (MPa)		
	$\alpha = 3.1$	α =3.0	$\alpha = 2.9$
0	1	1	1
0.004	12	12	13
0.018	54	56	58
0.031	91	94	97
0.041	120	124	129
0.050	147	152	157
0.060	177	183	190
0.070	206	212	220
0.080	236	244	252
0.090	265	274	284
0.100	295	305	351
0.104	307	317	328

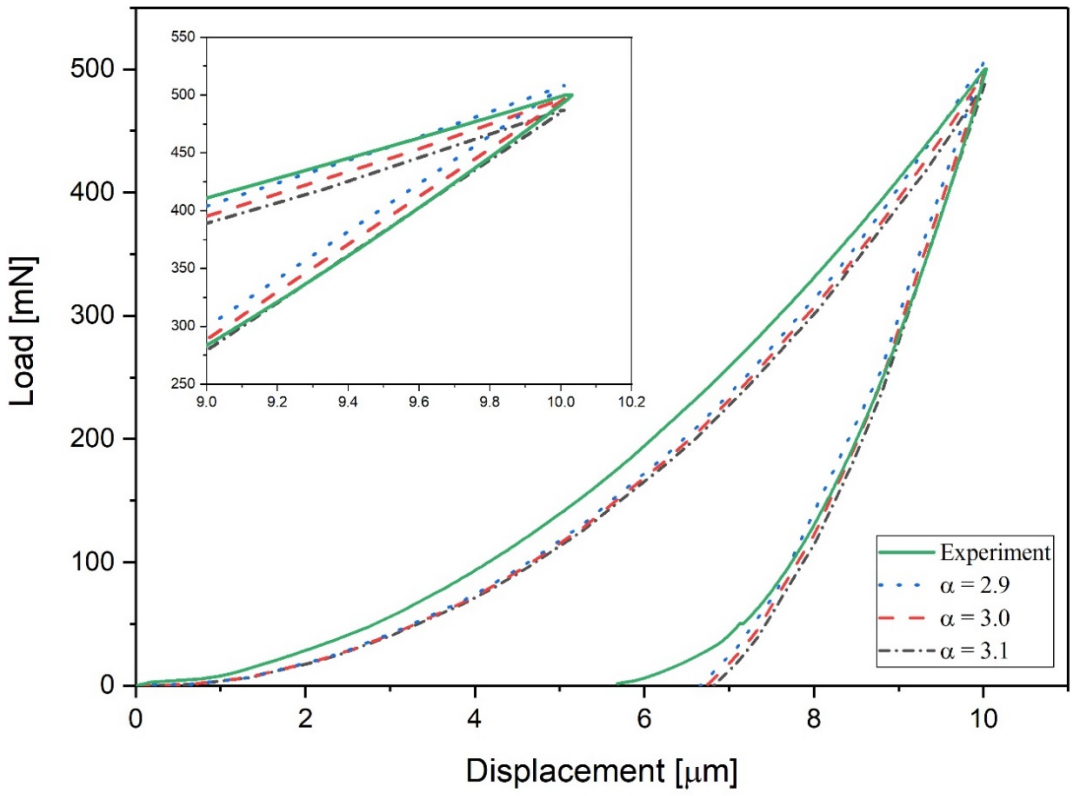

Figure S1.2. Loading-unloading curves with $h = 10\mu m$ from experiment and ABAQUS with different α.

S2. Mesh Convergence Study

Mesh size affects the solution accuracy in finite element method. However, finer mesh takes high computational resources. Different mesh sizes are considered to balance accurate results and computational resources. 1μm depth is chosen as an example to optimise the mesh size. Mises stress distributions with different mesh sizes are shown in Figure S2.1 along with an influence of mesh on the maximum von misses stress given in Table S2. In this case, an increase from 55206 to 80420 yields only a 3.65% increase in maximum von misses stress. The stresses on test specimen with 1μm depth are depicted in Figure S2.2, where convergent behaviour is observed.

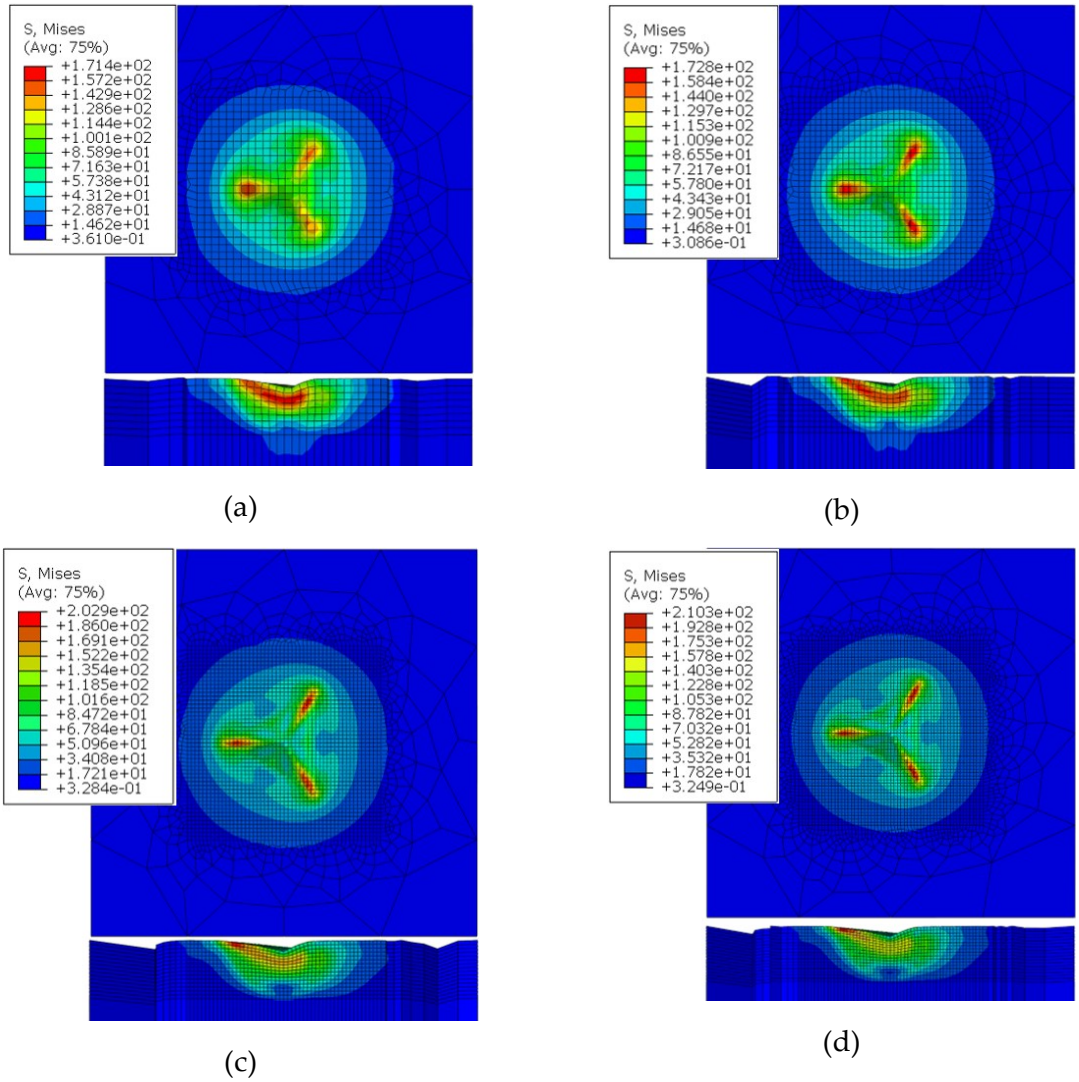

Figure S2.1. Contour von misses stress plot with depth=1μm for various meshes. **(a)** Mesh size = 0.4 μm. **(b)** Mesh size = 0.3 μm. **(c)** Mesh size = 0.2 μm. **(d)** Mesh size = 0.18 μm.

Table S2. Maximum von misses stress with depth h = 1μm: influence of mesh size

Mesh size (μm)	0.4	0.3	0.2	0.18
No. of element	10208	22046	55206	80420
An increase in element		11838	33160	25214
Max Von Mises Stress (MPa)	171.4	172.8	202.9	210.3
An increase in stress (%)		0.82	17.42	3.65

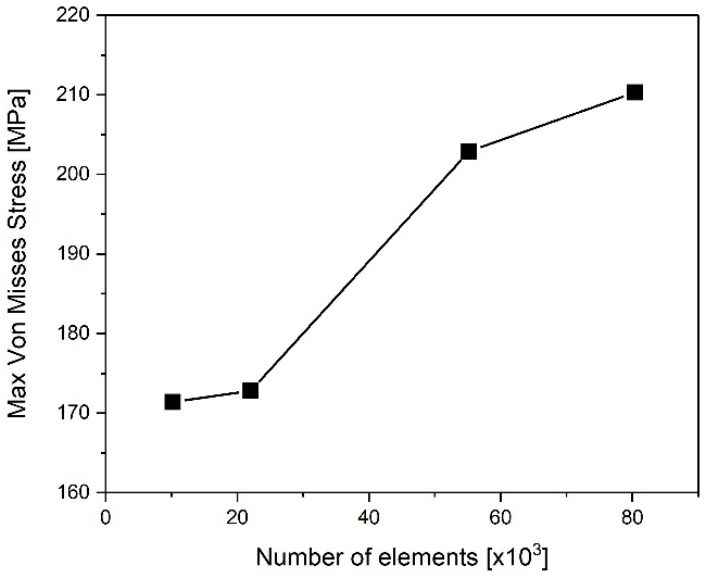

Figure S2.2. Stress sensitivity to number of elements.

Depths are measured from both the displacement of diamond tip and the block by ABAQUS comparing with experimental result depicted in Figure S2.3. The loading-unloading curves on tips from ABAQUS all match the curve from experiment due to the rigid tip. The displacement on block which influences most by the mesh should also satisfy experimental data. Considering different mesh sizes illustrates the displacement on block will fit the experimental result with mesh size smaller than 0.2 μm which is one fifth of the depth. Same as d=1μm, both d=5 μm and 1 μm with one fifth of the depth as the mesh size can obtain converge result in ABAQUS.

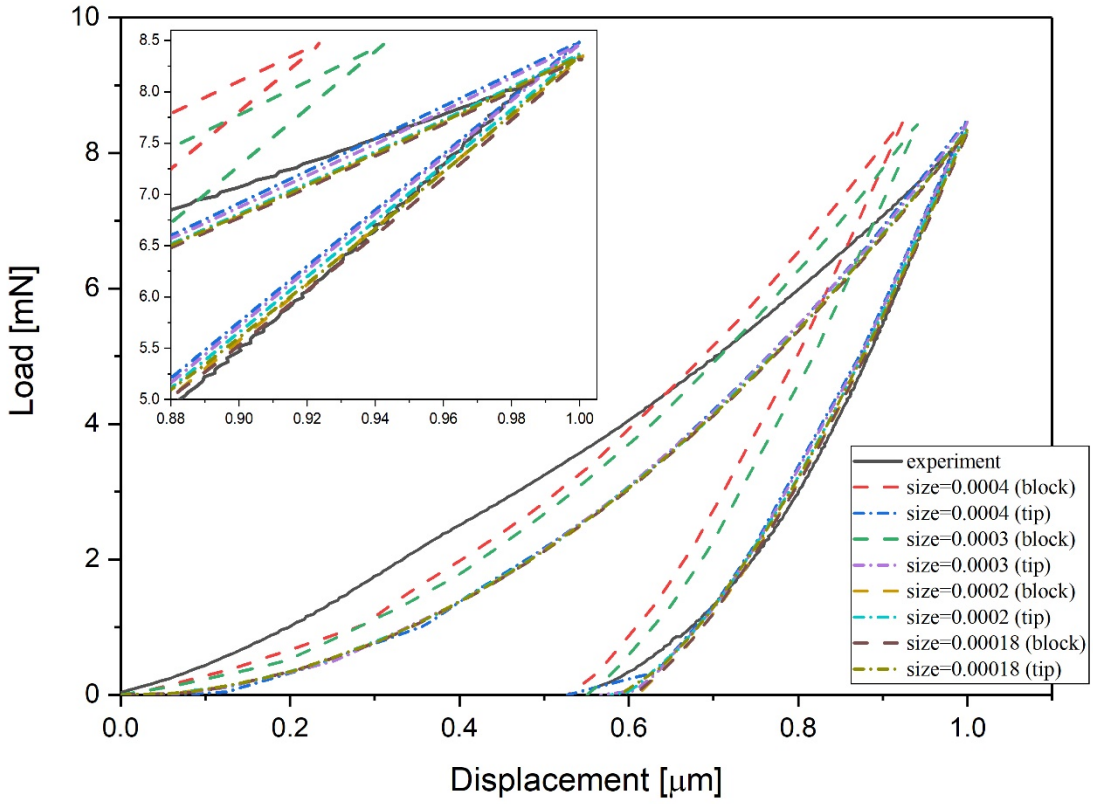

Figure S2.3. Loading-unloading curves from experiment and ABAQUS on both tip and block with different mesh size.

S3. Experiment Analysis of Indents in a Matrix for $h = 10\mu m$

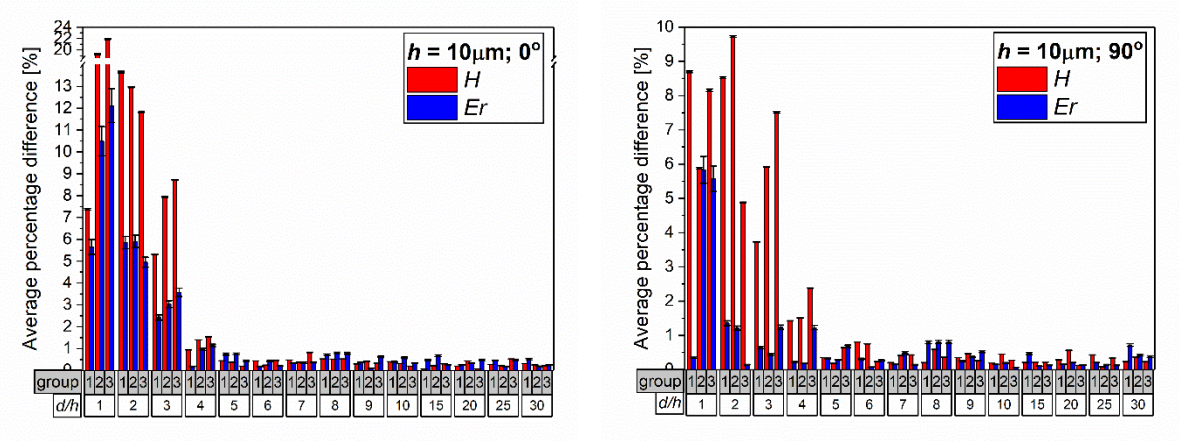

(a) (b)

Figure S3.1. Average percentage difference of Hardness and Modulus values for three indents within a group for various maximum indentation depth and separation. (a) orientation 0°, h = 10 μm; (b) orientation 90°, h = 10 μm.

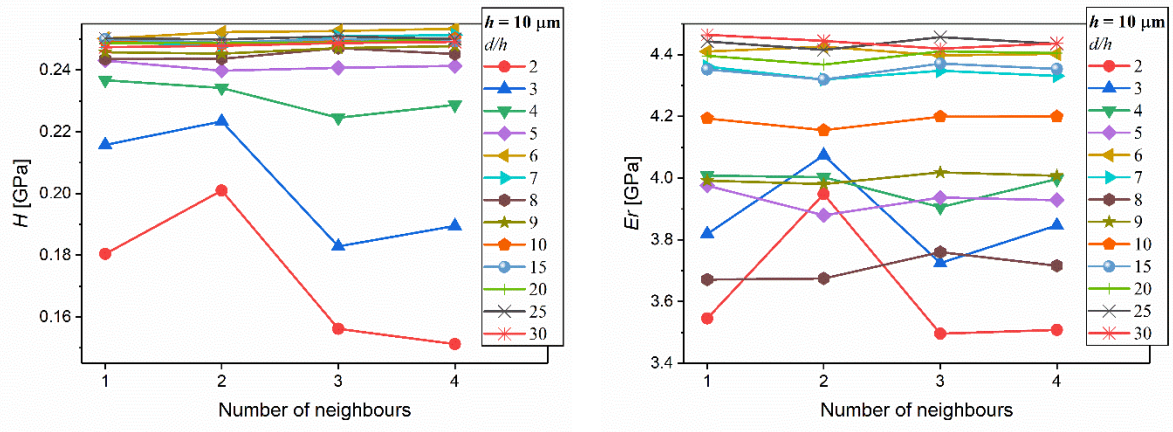

(a) (b)

Figure S3.2. (a) Hardness and (b) reduced modulus as a function of number of neighboring indents and spacing for maximum depth of 10 μm.

S4. Finite element analysis the maximum depth $h = 5\mu m$ and $10\mu m$ with three different orientations

The von misses stress contours for $h = 5\mu m$ and 10 μm from ABAQUS with different distance and orientation are depicted in Figures S4.1 and S4.2, respectively. The figures show the top view and cross-section, cut through the center of the max depth as indicated with a dotted line in the images in the first row. In the last row, a Von Misses stress vs depth taken from FEA cross-section at the center between two indents is provided. The depth in this case means the distance taken from the very top surface going towards the sample bulk. FEA analysis shows that the von misses stress and thus plastic zone would overlap until $d/h = 10$ for both maximum depth. At $d/h = 10$, there are still low stresses measured, and the full separation is at $d/h = 15$. It also confirmed that the stress value stays constant with $d/h = 15$ and above. This effect is independent of the maximum depth and tip orientation.

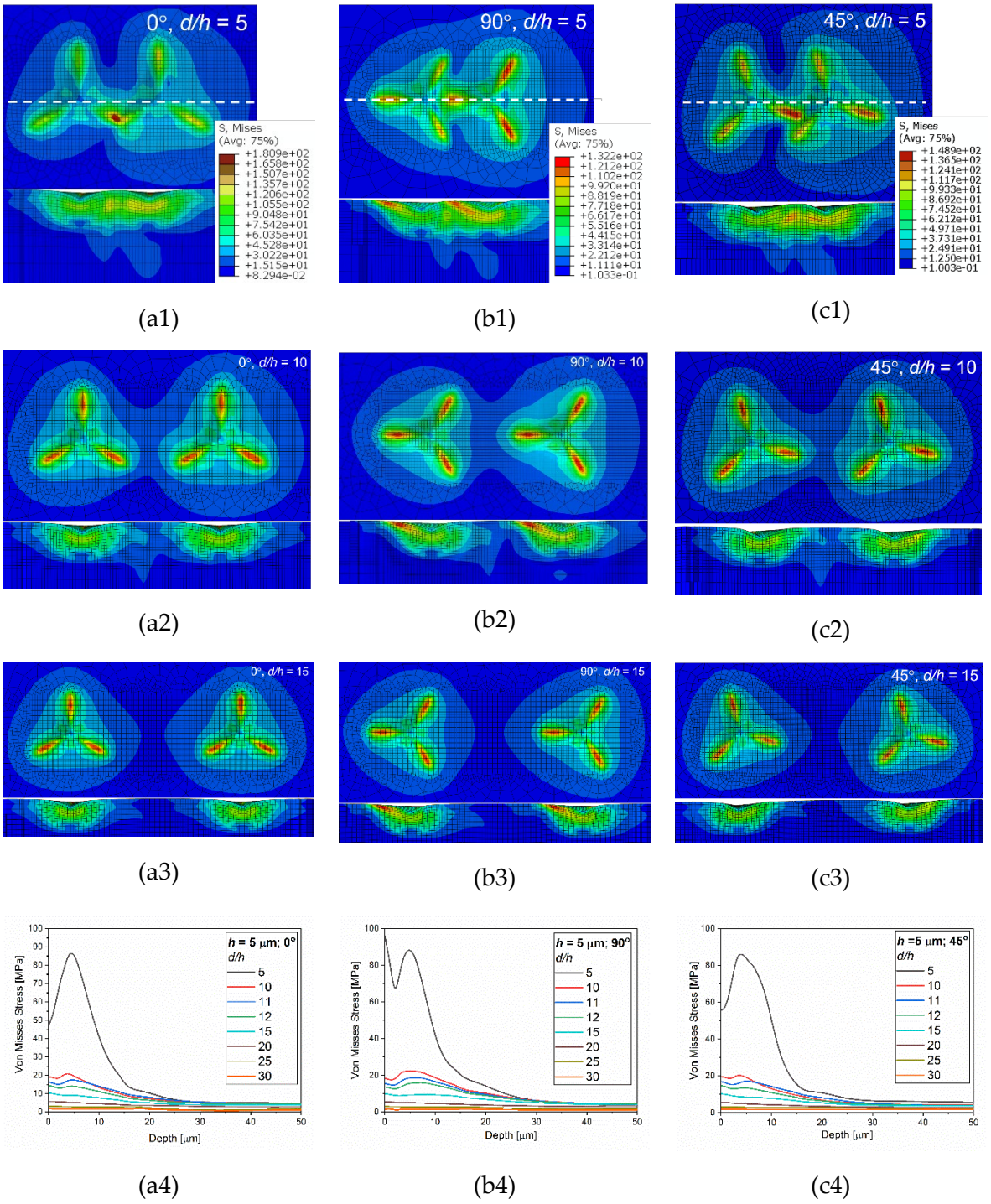

Figure S4.1. Von misses stress [MPa] distributions for h=5µm with different orientations and different nominal separations. **(a)** 0°, **(b)** 90° and **(c)** 45°; **(1)** d/h = 5, **(2)** d/h = 10, **(3)** d/h = 15 and **(4)** Von Misses stress vs depth taken from FEA cross-section at the centre between two indents.

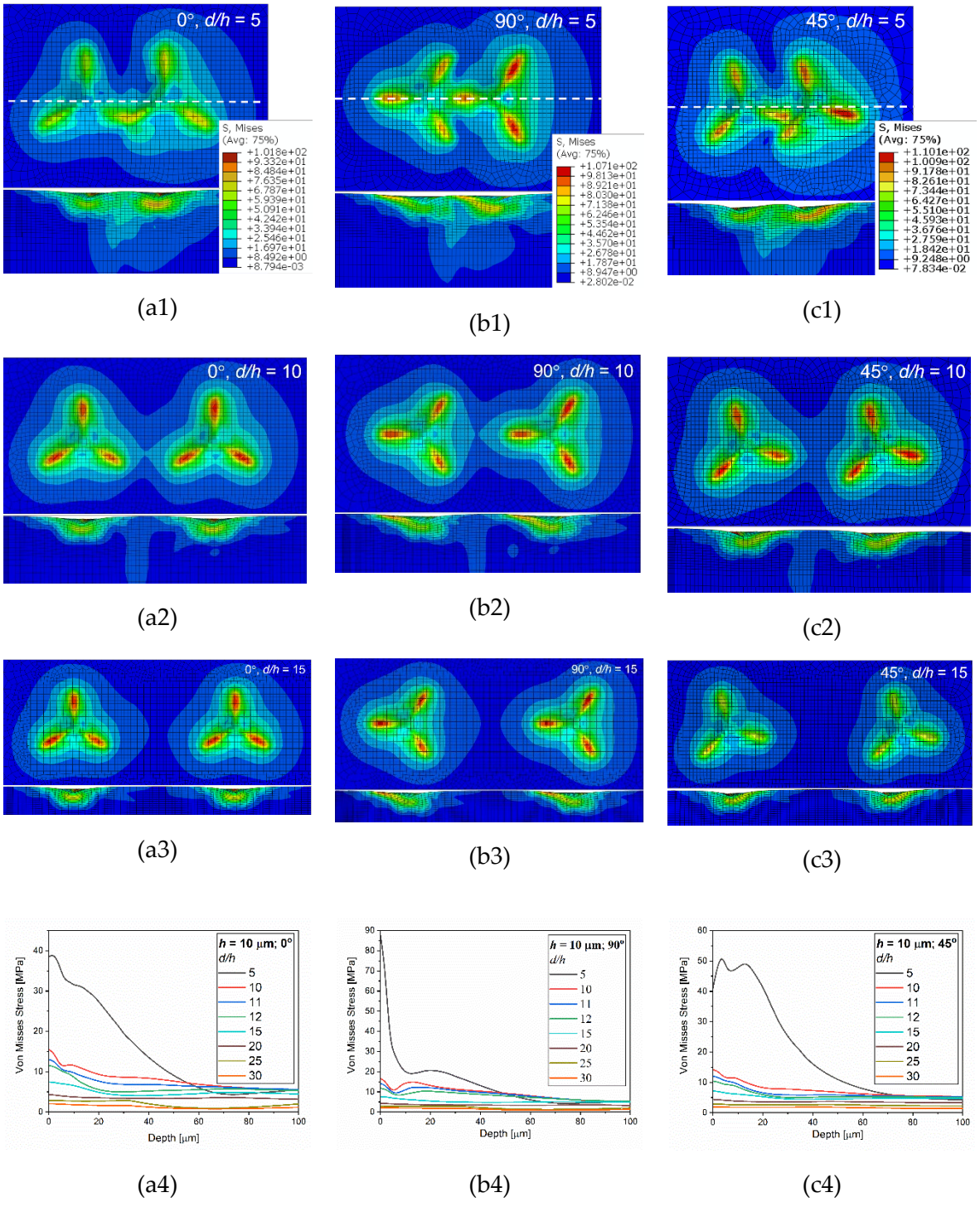

Figure S4.2. Von misses stress [MPa] distributions for h=10µm with different orientations and different nominal separations. **(a)** 0°, **(b)** 90° and **(c)** 45°; **(1)** d/h = 5, **(2)** d/h = 10, **(3)** d/h = 15 and **(4)** Von Misses stress vs depth taken from FEA cross-section at the centre between two indents.